RSC Advances

PAPER

View Article Online
View Journal | View Issue

Cite this: *RSC Adv.*, 2014, **4**, 45760

Large-scale fabrication of highly aligned poly(*m*-phenylene isophthalamide) nanofibers with robust mechanical strength†

Kun Chen,‡[a] Shichao Zhang,‡[a] Bowen Liu,[a] Xue Mao,[a] Gang Sun,[b] Jianyong Yu,[b] Salem S. Al-Deyab[c] and Bin Ding*[ab]

Received 31st July 2014
Accepted 5th September 2014

DOI: 10.1039/c4ra07901a

www.rsc.org/advances

Creating a facile and efficient method that can provide large-scale, highly aligned, and high strength nanofibers has proved extremely challenging. This work responds to these challenges by designing and evaluating poly(*m*-phenylene isophthalamide) (PMIA) nanofibrous materials with robust mechanical strength, which can be fabricated on a large scale *via* a facile combination of relative humidity (RH)-regulated electrospinning and multi-level aggregate reconstructing. The morphology and structure of the PMIA membranes can be finely controlled by regulating the solution concentration and RH during spinning, and a possible RH-regulated alignment mechanism was proposed. Additionally, PMIA nanofibrous aggregates of yarns and subsequent plaits were built up by multi-level reconstructing. During the first-level reconstructing based on twisting, the structure and mechanical properties of the yarns can be facilely optimized by tuning the twist level, and the PMIA yarns with 3000 TPM possess robust tensile strength of 262 MPa. The second-level reconstructing based on yarns braiding endows the corresponding nano-plaits with the highest tensile strength of 330 MPa. This novel method provides a new insight into the design and development of highly aligned nanomaterials for various applications.

Introduction

Over the past decade, one dimensional nanofibers have drawn tremendous attention due to their small diameter, large surface area, and high porosity, which result in high efficiency in various application fields including the environment, energy, electronics, optics, and healthcare.[1,2] Compared with various approaches including drawing process, melt-blown method, and islands-in-a-sea process, electrospinning has been generally acknowledged as the most effective and versatile technology for producing nanofibers with controlled dimensions, fiber morphology and functional components.[3] The electrospun nanofibers, in particular, are of great interest owing to their controllable structures, unique functionalities, and array of potential applications as protective clothing, filters, sensors, separators, and structural materials.[4,5] So far, various nanofibers electrospun from numerous polymer systems, including homopolymers, copolymers, blends, and composites, have been successfully prepared. However, the inherent limits of mechanical property, combined with poor processability for physical manipulation of weaving and knitting, have raised the concern whether the nanofibers can ever be truly applied for practical application.[6,7]

Up to now, substantial strategies have been established to enhance the mechanical properties of electrospun nanofibers, including geometric arrangement,[8] physical doping,[9] chemical modification,[10] post treatment,[11] *etc.* Among them, aligning strategies offer distinct advantages in terms of feasibility, practicability, efficiency, and economy. In view of above characteristics, considerable efforts have been devoted for fiber aligning to improve the mechanical strength of nanofibers. Existing strategies for fabricating aligned electrospun nanofibers aggregated in the form of membranes or yarns, can be divided into two categories: modifying the spinning devices[12–19] and optimizing solution properties.[20–23]

Various methods based on modifying the spinning devices have been built up for collecting aligned nanofibers in the past decade, such as high speed disc collecting,[12] gap or gaplike substrate collecting,[13,14] field-assisted spinning,[15] conjugate spinning,[16] *etc.* These methods are useful to produce aligned fibers, however, some drawbacks still remain. For example, the sharp edge disc and parallel electrodes techniques work well at producing highly aligned fibers, but the resulting materials are

[a]*State Key Laboratory for Modification of Chemical Fibers and Polymer Materials, College of Materials Science and Engineering, Donghua University, Shanghai 201620, China. E-mail: binding@dhu.edu.cn*

[b]*Key Laboratory of Textile Science & Technology, Ministry of Education, College of Textiles, Donghua University, Shanghai 201620, China*

[c]*Petrochemical Research Chair, Department of Chemistry, College of Science, King Saud University, Riyadh 11451, Saudi Arabia*

† Electronic supplementary information (ESI) available: Compositions and properties of solutions, alignment degree of PMIA membranes, TGA curves. See DOI: 10.1039/c4ra07901a

‡ These authors have contributed equally to this work.

not applicable for most of the applications because of their seriously limited quantity and size. The technique assisted by magnetic field or gas flow field does not offer so high alignment degree as desired to the membranes, exhibiting an obstacle to significantly improving the mechanical strength of nanofibers. Although the nanofibrous yarns can be directly produced by the special apparatus (water reservoir collectors,[17] funnel shape collectors,[18] oppositely charged nozzles,[19] *etc.*) during spinning, they have fatal defects of low productivity, weak mechanical properties, and poor reproducibility for the practical application.

On the other hand, few efforts have been devoted to producing aligned nanofibers by solely optimizing solution properties, including the regulation of solvent dielectric properties,[20] viscosities,[21] additives,[22] and conductivities.[23] These methods overcome the limitations of sophisticated devices, providing a relatively facile technique for aligning fibers on a large scale. However, the resulting membranes or yarns still suffer from relatively low alignment and weak mechanical property. For instance, the aligned polyethersulfone nanofibers prepared by salt-induced pulse electrospinning only have a tensile strength of 26.89 Mpa,[22] while continuous yarns prepared by self-bundling electrospinning method based on optimizing solution conductivity cannot satisfy the needs of practical applications due to their low productivity and poor reproducibility.[23]

The poly(*m*-phenylene isophthalamide) (PMIA), also known as one of the three high performance fibrous materials, proved to be an ideal candidate for fabricating high strength nanofibers. One-dimensional PMIA nanofibers, in particular, have attracted much attention in recent years, due to their array of potential applications as protective clothing, high-temperature filters, electrical insulating materials, supercapacitors, and nanocomposite materials, which can be attributed to their unique structure and functionalities.[5,23] Previously, the hierarchically aligned PMIA/multi-walled carbon nanotube (MWCNT) hybrid nanofibers with a tensile strength of 316.7 MPa were prepared in our group.[24] In view of that the robust tensile strength mainly depend on the addition of MWCNT, keeping such high tensile strength for PMIA/MWCNT fibers, especially during large-scale fabrication, is still a great challenge owing to the limitation on dispersibility of MWCNT and stability of spinning solution. To the best of our knowledge, there have been no previous reports on the development of the fibers aligning and aggregates reconstructing for large-scale fabrication of high strength nanofibrous materials.

Herein, we present the large-scale fabrication of highly aligned PMIA nanofibers with robust mechanical strength *via* RH-regulated electrospinning and multi-level aggregates reconstructing. The structure and mechanical property of PMIA membranes were finely controlled by regulating solution concentration and RH during spinning. Moreover, the structure and mechanical property of yarns were thoroughly investigated by tuning the twist level, and the thermal tolerance of yarns with optimum twist level was systematically evaluated. Additionally, a multi-level structured nano-plait with robust tensile strength was also successfully fabricated.

Experimental

Materials

Initial PMIA fibers (Teijinconex®) were purchased from TEIJIN Co., Ltd., Japan. Lithium chloride (LiCl) and dimethylacetamide (DMAc) were supplied by Shanghai Chemical Reagents Co., Ltd., China. All chemicals were of analytical grade and were used as received without further purification.

Preparation of PMIA solutions

PMIA solutions were prepared using initial PMIA fibers, LiCl, and DMAc as starting materials by a vigorous stirring process. Firstly, the LiCl was vacuum-dried at 120 °C for 3 h, and the LiCl/DMAc ionic liquid was prepared by dissolving 2 wt% dried LiCl in DMAc solvent with magnetically stirring for 3 h at the room temperature. Then 7.5, 10, 12.5, and 15 wt% initial PMIA fibers which were dried at 120 °C for 2 h in the vacuum oven were added into the LiCl/DMAc ionic liquid with vigorous stirring for 24 h at 80 °C to be completely dissolved. The detailed compositions and properties of relevant solutions were shown in Table S1 in the ESI.†

Fabrication of PMIA nanofibrous membranes

The large-scale PMIA membranes were collected on a rotating drum by electrospinning, as shown in Fig. 1a. The process was performed by using the DXES-3 spinning equipment purchased from Shanghai Oriental Flying Nanotechnology Co., Ltd., China. Typically, the PMIA solutions were transferred into 10 mL plastic syringes for electrospinning at 25 kV keeping a tip-to-collector distance of 20 cm. The positive electrode of the high voltage power supply was attached to the metal needle tip while the grounded stainless drum (length of 50 cm, diameter of 25 cm) was used as the collector wrapped with copper mesh and rotated at 500 rpm. The feeding rate of the PMIA solutions by the syringe pump was 0.1 mL h^{-1} throughout. The ambient temperature was 25 °C, and the RH was adjusted to 35%, 45%, 55%, and 65% by using a CH948B humidity controller (WGI Inc., USA).

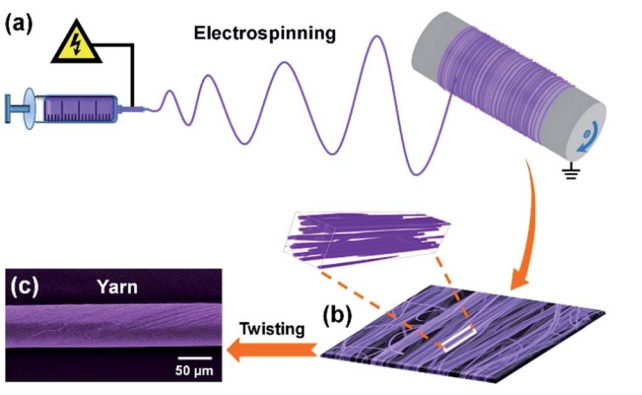

Fig. 1 (a) Schematic diagram illustrating the fabrication of PMIA nanofibrous membranes deposited on grounded rotating roller. (b) Illustration of the concept of highly aligned PMIA membranes. (c) FE-SEM image of PMIA nanofibrous yarn.

The highly aligned electrospun PMIA nanofibrous strips for mechanical strength comparison were collected by a high speed rotating disc. The electrospinning process was performed under the same conditions mentioned above except the disc collector and the tip-to-collector distance of 5 cm. This grounded stainless disc collector had a diameter of 30 cm and a disc rim of 1 cm and rotated at 3000 rpm. The ambient temperature was 25 °C, and the RH was 55%. All the samples were vacuum-dried at 80 °C for 2 h to remove the residual solvent.

Fabrication of PMIA nanofibrous yarns and nano-plaits

The first-level nanofibrous aggregates reconstructing based on twisting was proposed to fabricate PMIA yarns from the highly aligned membranes, as depicted in Fig. 1b and c. Firstly, the electrospun PMIA membranes with the identical thickness of 3 ± 0.1 μm were gently cut into ribbon-shaped belts with a length of 13 cm and a width of 3 mm using a rotary cutter. Then various twist levels of 1000, 2000, 3000, and 4000 twists per meter (TPM) was introduced into the belts by a yarn twisting apparatus (Y331A, Changzhou Dahua Electronics Instruments Co., Ltd., China), which had a meter for controlling the number of rotations. And, the distance between the chucks (fixed clamp and rotary clamp) was fixed at 10 cm. The second-level nanofibrous aggregates reconstructing was performed under a magnifying glass, and the nano-plait was created by braiding three yarns with an optimum twist level of 3000 TPM.

Characterization

The morphology of membranes and yarns were observed by field emission scanning electron microscopy (FE-SEM) (S-4800, Hitachi Ltd., Japan) after being coated with carbon for 5 min. The fiber diameter and its distribution of each membrane were measured by an image analyzer (Adobe Photoshop CS2). At least 100 fibers were randomly used to determine the average fiber diameter for each sample. The viscosity, conductivity, and surface tension of the PMIA solutions were measured using a viscometer (SNB-1A, Shanghai Fangrui Instrument Co., Ltd., China), a conductivity meter (FE30, Mettler-Toledo Group, Switzerland), and a surface tension meter (QBZY-1, Shanghai Fangrui Instrument Co., Ltd., China), respectively. The thickness of samples was measured by a thickness gauge (CHY-C2, Labthink Co., Ltd., China) for five times independently, and the average value was obtained. The mechanical property of the membranes and yarns were tested on a tensile tester (XQ-1C, Shanghai New Fiber Instrument Co., Ltd., China) with a crosshead speed of 5 mm min^{-1}. The size of the membrane specimen for test was 3×20 mm and ten specimens from each membrane were tested for tensile behavior. To characterize fiber alignment, vertical lines were drawn in FE-SEM images, angles between the fibers and the vertical lines were measured by an image analyzer (Adobe Photoshop CS2), and were defined as fiber angles. Histograms of these fiber angles were plotted over the $-90°$ to $+90°$ range by $5°$ interval. The degree of alignment ($DOA_{\pm 10}$) was defined as the percentage of fibers within $\pm 10°$ of the alignment direction, similarly, $DOA_{\pm 20}$ was for $\pm 20°$. At least 100 fiber angles were measured from each FE-SEM image for above calculations. The yarn diameters were measured by a high-precision microscope with an image analyzer (BH2-UMA, OLYMPUS, Japan). Thermogravimetric analysis (TGA) of PMIA nanofibrous yarns was performed on a thermogravimetric analyzer (TG209F1, NETZSCH, Germany) from 30 to 500 °C with a heating rate of 10 °C min^{-1} in air atmosphere.

Results and discussion

Morphology of PMIA nanofibrous membranes

The representative FE-SEM images of PMIA nanofibers from various concentrations were presented in Fig. 2a–d, revealing the fibers randomly deposited as three-dimensional structures in the form of nonwoven mats. Fig. 2a showed that the nanofibers fabricated from 7.5 wt% PMIA solution exhibited a structure with few beads and an average diameter of 63 nm. While the average diameter of membranes from 10, 12.5, 15 wt% PMIA solutions were 137, 148, 190 nm, respectively, indicating that further increasing the solution concentration has significantly increased the average diameter of PMIA fibers (Fig. 2e). This change could be a consequence of the obviously increased viscosity and decreased conductivity of the solution, as shown in Table S1,† which both could greatly weaken the stretching of fluid jets during electrospinning.[25]

To further investigate the effect of solution concentration on the mechanical property of PMIA membranes, tensile strength of various membranes were demonstrated in Fig. 2f. The relevant membranes from PMIA solution of 7.5, 10, 12.5, and 15 wt% possessed the tensile stress of 25, 55, 64, and 98 MPa, respectively, indicating a regular increase of tensile strength

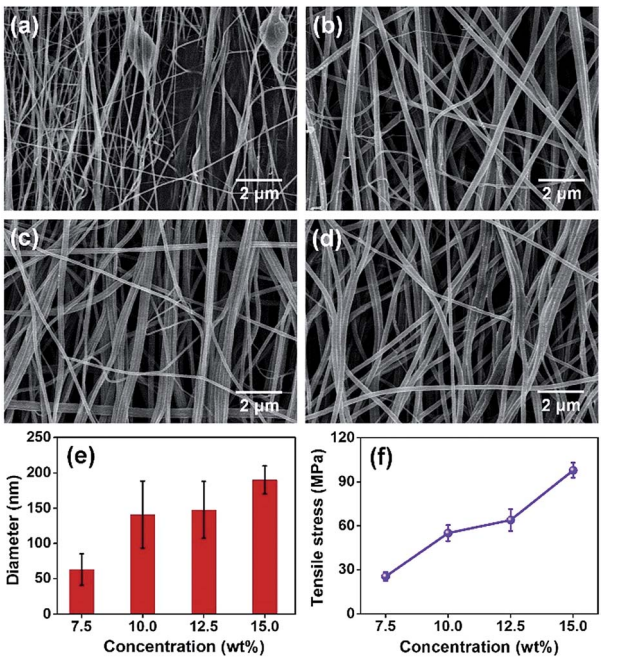

Fig. 2 FE-SEM images of PMIA nanofibrous membranes formed with PMIA concentration of (a) 7.5, (b) 10, (c) 12.5, and (d) 15 wt%. Average fiber diameters (e) and tensile stresses (f) of relevant membranes.

upon increasing the solution concentration. This significant enhancement of the mechanical property was mainly due to the transition of nanofibers uniformity including beads-on-string structure[26] and fiber diameter distribution.[27] The membrane from 7.5 wt% PMIA solution showed the lowest tensile strength of 25 MPa, while further increasing the concentration has greatly increased the strength, which could be attributed to the no-beads structure. Furthermore, careful analysis of FE-SEM images (Fig. 2b–d) revealed that the amount of nanowires with diameters of < 30 nm reduced with the increasing solution concentration, resulting in the decreased standard deviation of fiber diameter, as shown in Fig. 2e. The nanowires would break easily and quickly during the tensile test, resulting in the further collapses of the rest fibers in the membranes. While, the uniform structure could ensure that the fiber breakage occurred at almost the same time, which was of great benefit to reduce the chance of generation and extension of the cracks.[27–29]

Effect of RH on the alignment of PMIA nanofibers

The alignment of PMIA nanofibers within membranes can be optimized by facilely regulating the RH during spinning. Fig. 3a–c presented the representative FE-SEM images of PMIA nanofibers obtained by varying the RH, exhibiting a remarkable change in the degree of alignment (DOA) of relevant nanofibers. The PMIA nanofibers from a low RH of 35% were randomly arranged ($DOA_{\pm 10} = 17.8\%$), which was caused by the bending and whipping movement of electrospinning jets, and further increasing the RH until 55% has significantly enhanced the aligned structure, as shown in Fig. S1.† The PMIA membranes fabricated at RH of 55% exhibited the highest alignment degree ($DOA_{\pm 10} = 97.8\%$, $DOA_{\pm 20} = 100\%$), which was much better than the ever reported data (*e.g.*, $DOA_{\pm 20} = 90\%$,[30] $DOA_{\pm 20} = 70\%$ (ref. 31)). This highly aligned structure was favorable to achieve a higher mechanical strength of 153 MPa for PMIA membranes. However, further increasing the RH to 65% has not only decreased the alignment degree of nanofibers ($DOA_{\pm 10} = 56.3\%$), but also changed the PMIA membranes to a fluffy structure, leading to a dramatic decrease in the mechanical strength (44 MPa), as demonstrated in Fig. 3c and d. The RH-regulated electrospinning proved to be a facile, effective, and economic way to restrict the chaotic path of the charged jets for controlling the alignment of the resulting nanofibers, without modifying the spinning device or optimizing solution properties.

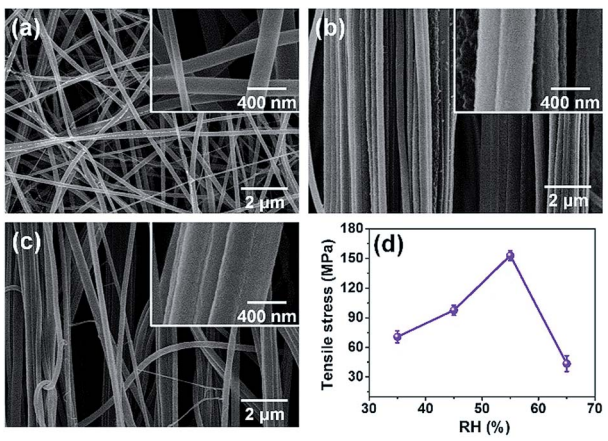

Fig. 3 FE-SEM images of PMIA nanofibrous membranes fabricated from 15 wt% PMIA solution at RH of (a) 35%, (b) 55%, and (c) 65%. (d) The tensile stress of relevant membranes.

RH-regulated aligning mechanism

The mechanism based on charge loss and phase separation can be used to elucidate how the alignment and mechanical property of PMIA nanofibers were affected by the RH during spinning, as illustrated in Fig. 4a. The PMIA is a strong hydrophilic polymer due to benzene–amide linkages in the skeletal chain, meanwhile, LiCl is water-soluble salt.[24] Therefore, the moisture in the air would play a significant role in the flying and solidifying process of electrospun jets, and finally affected the structure of resulting membranes. The optical images in Fig. 4b–e clearly showed that the whipping instability region narrowed initially with increasing the RH until 55% and then broadened during electrospinning.

The interesting phenomenon mentioned above can be explained by several possible reasons.[32–34] From the point of view of charge loss, higher RH results in more water molecules around the flying jets, which can decrease the amount of excess charges on the jets due to molecular polarization and charge transfer.[32] Thus, the electrostatic repulsion between the charged jets decreases, leading to a narrowed whipping instability region. These results agree with previous work in which the DOA of PMIA nanofibers improved with increasing RH from 25% to 55%.[24] From phase separation viewpoint, water molecules which act as a nonsolvent to PMIA polymer, nucleate and condense on the surface of evaporating jets facilely with the benefit of the abundant hydrogen bond formed between the PMIA macromolecules and water molecules, then facilitate

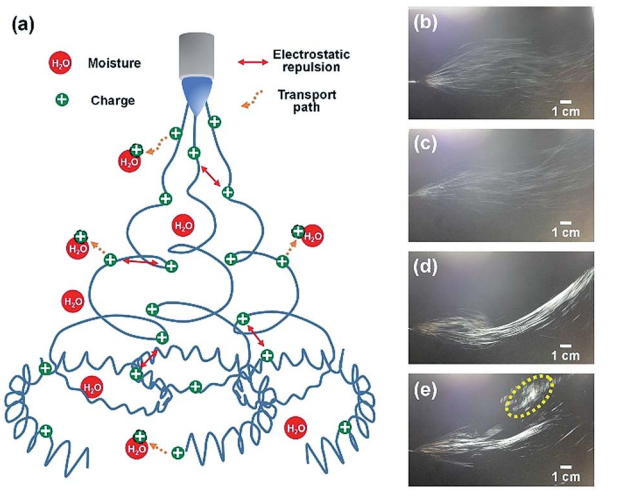

Fig. 4 (a) Schematic diagram illustrating the possible formation mechanism of nanofibers with different alignment degree during electrospinning process. Optical images of charged jet behavior at different RH of (b) 35%, (c) 45%, (d) 55%, and (e) 65%.

solidification of the fluid jets before they deposit on the drum surface, as shown in Fig. 4e (indicated by the dotted circle). Meanwhile, the accelerated solidification decreases the charge density of ejected jets.[33,34] As a consequence, the electrostatic force imposed to the jets becomes weaker, and then the resulting membranes exhibit a cotton-like structure indicating poor fiber–fiber internal friction under stretching. As expected, the fluffy structure formed at RH of 65% greatly deteriorates the mechanical strength (43.4 MPa) of PMIA membranes, as exhibited in Fig. 3d.

Effect of twist level on the structure and mechanical property of PMIA yarns

In order to further improve the mechanical property of PMIA nanofibers, the aggregates reconstructing based on twisting process was proposed to enhance the lateral interaction and friction between nanofibers. Fig. 5 presented the FE-SEM images of PMIA yarns with various twist levels, which were fabricated from PMIA membranes spun at RH of 55%. It is clearly showed that the increase of twist level of 1000, 2000, 3000, and 4000 TPM presented a remarkable decrease in yarn diameters of 109.6, 95.7, 80.7, and 78.5 μm, respectively, revealing that the critical twist level of 3000 TPM was enough to endow comparable compactness to the PMIA nanofibrous yarns. Meanwhile, the twist angle which was defined as the angle between the surface fibers and the yarn axis increased gradually from 17.6° to 32.8°, indicating an increasing obliquity of surface fibers. One interesting phenomenon was that, the alignment of surface fibers within yarns increased initially with increasing the twist level until 3000 TPM and then decreased, as shown in the insets of corresponding FE-SEM images. This phenomenon could be explained by the "climbing action" between adjacent fibers caused by excessive twisting.[35]

The representative stress–strain curves of various yarns displayed in Fig. 6 clarified the effect of twist level on the mechanical property of PMIA nanofibrous yarns. The PMIA

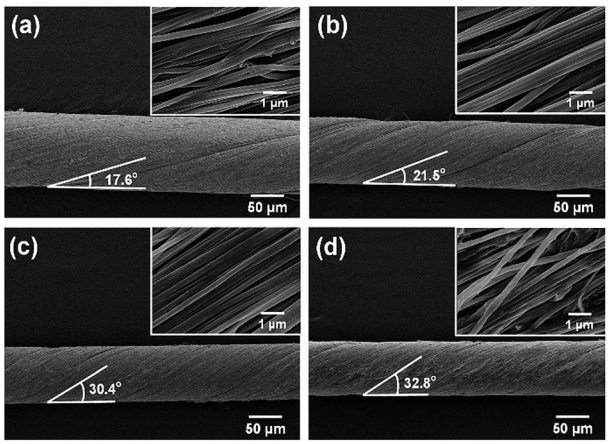

Fig. 5 FE-SEM images of PMIA yarns with various twist levels of (a) 1000, (b) 2000, (c) 3000, and (d) 4000 TPM fabricated from PMIA membranes spun from 15 wt% PMIA solution at RH of 55%. The insets are the images of surface morphology of corresponding yarns.

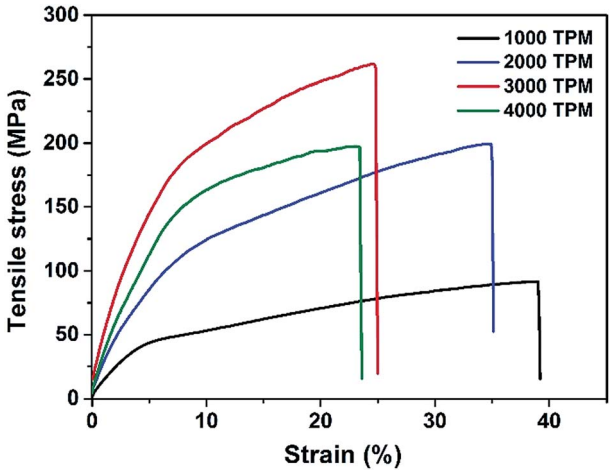

Fig. 6 Stress–strain curves of PMIA yarns with various twist levels.

yarns with twist level of 1000, 2000, 3000, and 4000 TPM possessed the tensile strength of 92, 199, 262, and 197 MPa, respectively, revealing that the tensile strength increased initially and then decreased with increasing twist level, which can be explained by that the interaction among nanofibers reached to the optimum state at 3000 TPM. While, the elongation at break continuously decreased from 39% to 23%.

Such interesting trends mentioned above can be elucidated by the two competitive effects of "fiber cohesion" and "obliquity effect", which changes to be the dominant factor in turn with the increasing twist level.[36,37] The tensile strength was determined by overall fiber tension resisting the breakage along the yarn axis, which was influenced by slippage and alignment of fibers within yarns. The transverse pressure and fiber twist angle increase simultaneously with the increasing twist level, the former could enhance interfiber friction and reduce fiber slippage to improve the tensile stress, while the latter weaken alignment degree and decreased the tensile stress.[36] As a result, at lower twist level stage (<3000 TPM), the fiber cohesion caused by increasing twist level was the main factor yielding intense local load sharing among fibers in the PMIA yarns, hence the maximum tensile stress was reached at 3000 TPM. Further increasing the twist level to 4000 TPM has turned the obliquity effect to be overwhelming. Consequently, component of fiber tension in the yarn axis direction reduced and tensile strength decreased. For the elongation at break of PMIA yarns, with the increasing twist level, nanofibers in yarns would suffer from a gradually enhanced stretch effect, resulting in a faster occurrence of fiber rupture among highly compacted yarns during the tensile test.[37]

Thermal tolerance of PMIA yarns

Herein, using the as-prepared PMIA nanofibrous yarns with 3000 TPM, we evaluated their thermal tolerance after annealing at various temperatures from 50 to 400 °C for 10 min. As shown in Fig. 7, the resulting yarns still exhibited robust tensile strength of 251 MPa up to 250 °C, then an obvious loss of strength occurred after the annealing treatment at 270 °C,

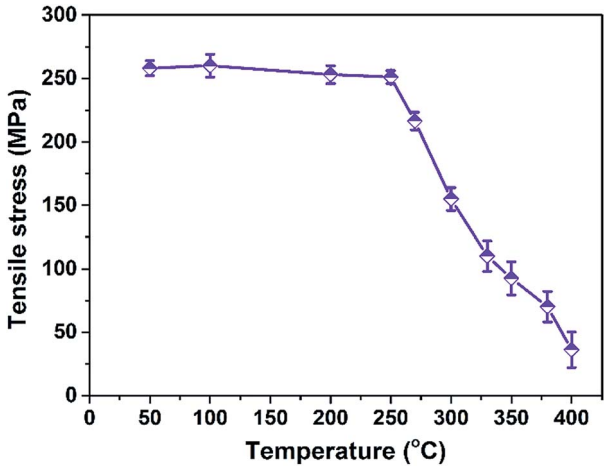

Fig. 7 Tensile stress of PMIA yarns with 3000 TPM annealed at various temperatures.

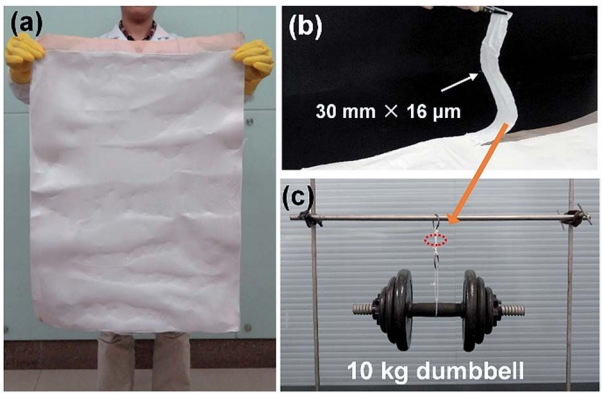

Fig. 8 (a) Photograph showing the large-scale (50 × 75 cm) of membrane consist of aligned PMIA nanofibers. (b) The strip with 30 mm width and 16 μm thickness cut from as-prepared PMIA nanofibrous membranes. (c) Photograph showing the as-prepared PMIA nanofibrous strip supporting a 10 kg dumbbell.

which was in accord with the PMIA glass-transition temperature. By further increasing the annealing temperature, the yarns suffered a significant loss of strength, which was due to the broken of hydrogen bonds and crystallite structure in polymers under higher temperature.[38] Notably, the tensile stress of PMIA yarns could be maintained 36 MPa after annealing at 400 °C, even higher than the tensile strength of some conventional electrospun nanofibers, showing a striking mechanical robust and thermal tolerant properties.[39]

Evidence of the excellent thermal stability also came from thermogravimetric analysis, as displayed in Fig. S2.† The initial weight loss of 7.61% occurred roughly at the temperature lower than 150 °C, implying either volatile moisture or solvent residues were removed. Then a gradual weight loss process was observed from 150 to 440 °C, but the sharp weight loss of PMIA nanofibrous yarns was above the initial decomposition temperature (IDT) of 440.4 °C, which could be ascribed to the pyrolysis of fibers.[38]

Large-scale fabrication and mechanical performance comparison

Benefiting from the jet-driven method rather than collector-driven method, large-scale aligned PMIA nanofibrous membranes with robust mechanical property could be successfully prepared *via* RH-regulated electrospinning. As expected, a large scale (50 × 75 cm) of highly aligned membrane was prepared by using a 5 needles multi-jet electrospinning device, as shown in Fig. 8a. This result further illustrated that the RH regulation method was quite stable to realize larger scale industrial production of aligned nanofibrous materials by only enlarging the equipment. Furthermore, Fig. 8b and c demonstrated that the PMIA membrane with size of 30 mm width and 16 μm thickness could facilely load a weight of 10 kg at least, showing excellent mechanical property and usability, which are of great importance for practical applications.

As a further proof of concept, the comparison of mechanical strength of PMIA membranes and yarns fabricated by both a normal speed rotating drum (500 rpm) and a high speed rotating disc (3000 rpm) was presented in Fig. 9. It is clearly showed that the tensile stress of the PMIA membranes collected by the drum and high speed disc was 153 and 171 MPa, respectively, while the corresponding yarns possessed the almost identical mechanical strength of 262 and 268 MPa. The above results indicated that the large-scale fabrication of PMIA nanofibers with robust mechanical strength was achieved, without compromising the alignment degree of the fibers, *via* a facile combination of RH-regulated electrospinning and aggregates reconstructing.

Multi-level structured nano-plaits

To further verify the processability of PMIA nanofibrous yarns, a multi-level structured nano-plait have been created by braiding three yarns with the optimum twist level of 3000 TPM. As can be seen from Fig. 10, this novel nano-plait possessed the highest tensile strength of 330 MPa, which may be attributed to yarn–yarn complementary effect. Generally, the tensile response of yarns was very sensitive to microcracks and other micro defects

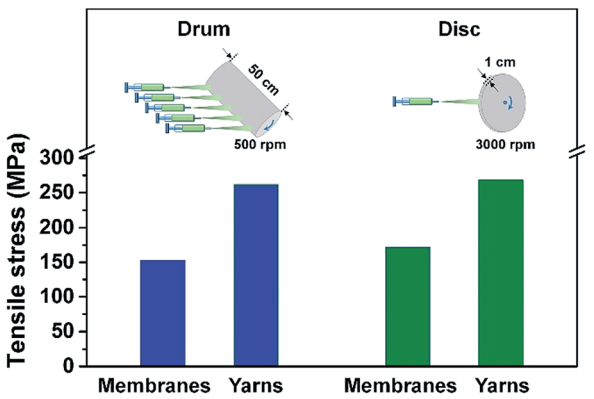

Fig. 9 Tensile stresses of membranes and yarns fabricated through drum and high speed disc, respectively.

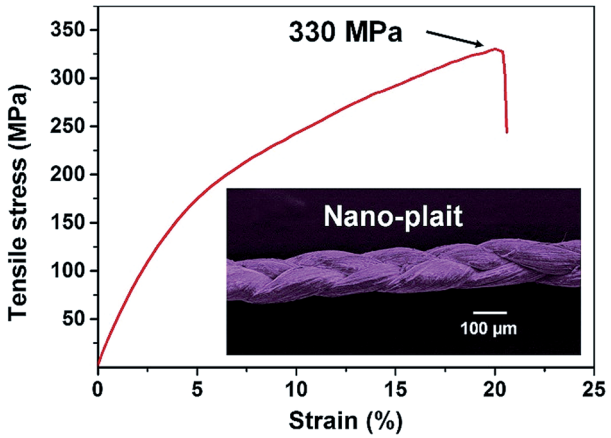

Fig. 10 Stress–strain curve of nano-plait braided from PMIA yarns with 3000 TPM.

during testing. Through braiding treatment, yarns within PMIA plait would arrange in a curved path, then the transverse forces built up among yarns under a stress load, indicating an enhanced lateral friction which can effectively decrease the stress concentration and suppress the deterioration of inherent defects of yarns.[40]

Conclusions

In summary, we have described the large-scale fabrication of highly aligned PMIA nanofibers with robust mechanical strength *via* RH-regulated electrospinning and multi-level aggregates reconstructing. The morphology and structure of PMIA membranes can be finely controlled by regulating the solution concentration and RH during spinning. The resulting PMIA membranes obtained at RH of 55% exhibited the highest $DOA_{\pm 10}$ of 97.8%, and a possible mechanism which consists of both charge loss and phase separation was first proposed to explain the formation of RH-regulated aligning. Moreover, based on the novel multi-level aggregates reconstructing including twisting and subsequent braiding, the as-prepared PMIA yarns with an optimum twist level of 3000 TPM showed robust tensile strength of 262 MPa and excellent thermal tolerance of 250 °C, while the multi-level structured nano-plaits possessed the highest tensile strength of 330 MPa. Consequently, the significant contribution of this work is that it provides not only an effective method for large-scale fabrication of highly aligned PMIA nanofibers with robust mechanical property, but also a versatile strategy for further design, development of aligned nanomaterials for various practical applications.

Acknowledgements

This work is supported by the National Basic Research Program of China (973 Program, 2011CB606103), the National Natural Science Foundation of China (51322304), the Program for New Century Talents of the University in China, the Fundamental Research Funds for the Central Universities, and the "DHU Distinguished Young Professor Program". The authors extend their appreciation to the deanship of scientific research at King Saud University for funding the work through the research group project no. RGP-089.

Notes and references

1 N. Bhardwaj and S. Kundu, *Biotechnol. Adv.*, 2010, **28**, 325.
2 S. Cavaliere, S. Subianto, I. Savych, D. Jones and J. Roziere, *Energy Environ. Sci.*, 2011, **4**, 4761.
3 K. Jayaraman, M. Kotaki, Y. Zhang, X. Mo and S. Ramakrishna, *J. Nanosci. Nanotechnol.*, 2004, **4**, 52.
4 B. Ding, M. Wang, X. Wang, J. Yu and G. Sun, *Mater. Today*, 2010, **13**, 16.
5 X. Tang, Y. Si, J. Ge, B. Ding, L. Liu, G. Zheng, W. Luo and J. Yu, *Nanoscale*, 2013, **5**, 11657.
6 Y. Long, M. Li, C. Gu, M. Wan, J. Duvail, Z. Liu and Z. Fan, *Prog. Polym. Sci.*, 2011, **36**, 1415.
7 M. Abbasipour and R. Khajavi, *Adv. Polym. Technol.*, 2013, **32**, E44.
8 D. Yang, B. Lu, Y. Zhao and X. Jiang, *Adv. Mater.*, 2007, **19**, 3702.
9 J. J. Ge, H. Hou, Q. Li, M. J. Graham, A. Greiner, D. H. Reneker, F. W. Harris and S. Z. D. Cheng, *J. Am. Chem. Soc.*, 2004, **126**, 15754.
10 L. Huang, J. T. Arena, S. S. Manickam, X. Jiang, B. G. Willis and J. R. McCutcheon, *J. Membr. Sci.*, 2014, **460**, 241.
11 X. Zhu, Q. Gao, X. Shi, Q. Pan, X. Jiang and R. Tao, *Adv. Mater. Res.*, 2011, **175–176**, 121.
12 S. Chen, P. Hu, A. Greiner, C. Cheng, H. Cheng, F. Chen and H. Hou, *Nanotechnology*, 2008, **19**, 015604.
13 N. Sharma, S. J. McKeown, X. Ma, D. J. Pochan and S. G. Cloutier, *ACS Nano*, 2010, **4**, 5551.
14 Y. F. Yao, Z. Z. Gu, J. Z. Zhang, C. Pan, Y. Y. Zhang and H. M. Wei, *Adv. Mater.*, 2007, **19**, 3707.
15 Y. Liu, X. Zhang, Y. Xia and H. Yang, *Adv. Mater.*, 2010, **22**, 2454.
16 H. Pan, L. Li, L. Hu and X. Cui, *Polymer*, 2006, **47**, 4901.
17 M. Yousefzadeh, M. Latifi, W.-E. Teo, M. Amani-Tehran and S. Ramakrishna, *Polym. Eng. Sci.*, 2011, **51**, 323.
18 A. M. Afifi, S. Nakano, H. Yamane and Y. Kimura, *Macromol. Mater. Eng.*, 2010, **295**, 660.
19 S.-H. Wu and X.-H. Qin, *Mater. Lett.*, 2013, **106**, 204.
20 S. Zaicheng, J. M. Deitzel, J. Knopf, C. Xing and J. W. Gillespie Jr, *J. Appl. Polym. Sci.*, 2012, **125**, 2585.
21 H. Yuan, S. Zhao, H. Tu, B. Li, Q. Li, B. Feng, H. Peng and Y. Zhang, *J. Mater. Chem.*, 2012, **22**, 19634.
22 Q. Zhang, L. Wang, Z. Wei, X. Wang, S. Long and J. Yang, *J. Polym. Sci., Part B: Polym. Phys.*, 2012, **50**, 1004.
23 X. Wang, K. Zhang, M. Zhu, H. Yu, Z. Zhou, Y. Chen and B. S. Hsiao, *Polymer*, 2008, **49**, 2755.
24 X. Wang, Y. Si, J. Yang, B. Ding, L. Chen, Z. Hu and J. Yu, *Nanoscale*, 2013, **5**, 886.
25 N. Wang, A. Raza, Y. Si, J. Yu, G. Sun and B. Ding, *J. Colloid Interface Sci.*, 2013, **398**, 240.

26 S. Moon, B.-Y. Ryu, J. Choi, B. Jo and R. J. Farris, *Polym. Eng. Sci.*, 2009, **49**, 52.
27 A. Baji, Y.-W. Mai, S.-C. Wong, M. Abtahi and P. Chen, *Compos. Sci. Technol.*, 2010, **70**, 703.
28 Y. Li, W. Xiao, K. Xiao, L. Berti, J. Luo, H. P. Tseng, G. Fung and K. S. Lam, *Angew. Chem., Int. Ed.*, 2012, **51**, 2864.
29 M. Karahan and N. Karahan, *Text. Res. J.*, 2010, **80**, 880.
30 K. Zhang, W. Jinglei, C. Huang and X. Mo, *Macromol. Mater. Eng.*, 2013, **298**, 565.
31 F. Wang, Z. Li, K. Tamama, C. K. Sen and J. Guan, *Biomacromolecules*, 2009, **10**, 2609.
32 L. Huang, N.-N. Bui, S. S. Manickam and J. R. McCutcheon, *J. Polym. Sci., Part B: Polym. Phys.*, 2011, **49**, 1734.
33 S. Tripatanasuwan, Z. Zhong and D. H. Reneker, *Polymer*, 2007, **48**, 5742.
34 X. Wang, B. Ding, G. Sun, M. Wang and J. Yu, *Prog. Mater. Sci.*, 2013, **58**, 1173.
35 X. Sui, E. Wiesel and H. D. Wagner, *Polymer*, 2012, **53**, 5037.
36 Y. Zhou, J. Fang, X. Wang and T. Lin, *J. Mater. Res.*, 2011, **27**, 537.
37 H. Yan, L. Liu and Z. Zhang, *Mater. Lett.*, 2011, **65**, 2419.
38 L. Yao, C. Lee and J. Kim, *Fibers Polym.*, 2010, **11**, 1032.
39 D. Blond, W. Walshe, K. Young, F. M. Blighe, U. Khan, D. Almecija, L. Carpenter, J. McCauley, W. J. Blau and J. N. Coleman, *Adv. Funct. Mater.*, 2008, **18**, 2618.
40 S. Rebouillat, B. Steffenino and A. Miret-Casas, *J. Mater. Sci.*, 2010, **45**, 5378.